Antisymmetric tensor unparticle and the radiative lepton flavor violating decays

E. O. Iltan, *
Physics Department, Middle East Technical University
Ankara, Turkey

Abstract

We study the contribution of the tensor unparticle mediation to the branching ratios of the radiative lepton flavor violating decays and predict a restriction region for free parameters of the scenario by using experimental upper limits. We observe that the branching ratios of the radiative lepton flavor violating decays are sensitive to the fundamental mass scales of the scenario and to the scale dimension of antisymmetric tensor unparticle. We obtain a more restricted set for the free parameters in the case of the $\mu \to e\gamma$ decay.

*E-mail address: eiltan@metu.edu.tr

The radiative lepton flavor violating (LFV) decays $l_i \to l_j \gamma$ reach great interest since their branching ratios (BRs) in the framework of standard model (SM) are much below the experimental upper limits, and, therefore, they are candidates to search and to test more fundamental models beyond. The current experimental upper limits of the BRs read BR $(\mu \to e\gamma) = 2.4\,(1.2) \times 10^{-12}\,(10^{-11})\,(\ 90\%CL)$ [1] ([2]), BR $(\tau \to e\gamma) = 3.3 \times 10^{-8}\,(\ 90\%CL)$ [3] and BR $(\tau \to \mu\gamma) = 4.4 \times 10^{-8}\,(\ 90\%CL)$ [3]. There is an extensive theoretical work in the literature in order to enhance BRs of these decays. They were studied in the SM with the extended Higgs sector, so called two Higgs doublet model (2HDM) [4]-[10], in supersymmetric models [11]-[18], in a model independent way [19], in the framework of the 2HDM and the supersymmetric model [20], in the SM including effective operators coming from the possible unparticle effects [21]-[22], in little Higgs models [23]- [26], in seesaw models [27] -[30], in models with A(4) and S(4) flavor symmetries [31], using the effective field theory with Higgs mediation [32], in the Higgs triplet model [33], in the framework of Higgs-induced lepton flavor violation [34].

In the present work, we consider the contribution of the antisymmetric tensor unparticle mediation to the BRs of the radiative LFV decays (see [35] for the contribution of the antisymmetric tensor unparticle mediation to the muon anomalous magnetic dipole moment, to the electroweak precision observable S, its effects in Z invisible decays and see [36] for the contribution of the antisymmetric tensor unparticle mediation to the lepton electric dipole moment). Unparticles [37, 38], being massless due to the scale invariance and having non integral scaling dimension d_U around the scale $\Lambda_U \sim 1.0\,TeV$, come out with the interaction of SM-ultraviolet sector at some scale M_U:

$$\mathcal{L}_{eff} = \frac{C_n}{M_U^{d_{UV}+n-4}}\, O_{SM}\, O_{UV}\,, \tag{1}$$

where d_{UV} is the scaling dimension of the UV operator [39]. Around the scale Λ_U the effective interaction becomes [40]

$$\mathcal{L}_{eff} = \frac{C_n^i}{\Lambda_n^{d_U+n-4}}\, O_{SM,i}\, O_U\,. \tag{2}$$

Here $O_{SM,i}$ is type i SM operator, n is its scaling dimension and Λ_n is the mass scale (see [35, 40] for details) which reads

$$\Lambda_n = \left(\frac{M_U^{d_{UV}+n-4}}{\Lambda_U^{d_{UV}-d_U}}\right)^{\frac{1}{d_U+n-4}}\,. \tag{3}$$

The antisymmetric tensor unparticle mediation induces these LFV decays at tree level and we consider the case that the scale invariance is broken at some scale μ after the electroweak

symmetry breaking (see for example [41, 42] for a possible interaction which causes that scale invariance is broken). The effective lagrangian [35] which can drive the radiative LFV decays is

$$\begin{aligned}\mathcal{L}_{eff} &= \frac{g'\,\lambda_B}{\Lambda_2^{d_U-2}}\,B_{\mu\nu}\,O_U^{\mu\nu} + \frac{g\,\lambda_W}{\Lambda_4^{d_U}}\,(H^\dagger\,\tau_a\,H)\,W_{\mu\nu}^a\,O_U^{\mu\nu} \\ &+ \frac{\lambda_{ij}}{\Lambda_4^{d_U}}\,y_{ij}\,\bar{l}_i\,H\,\sigma_{\mu\nu}\,l_j\,O_U^{\mu\nu}\,, \end{aligned} \tag{4}$$

where $l_{i(j)}$ is the lepton field, H is the Higgs doublet, g and g' are weak couplings, λ_B, λ_W and λ_{ij} are the unparticle-field tensor and unparticle-lepton-lepton couplings, $B_{\mu\nu}$ is the field strength tensor of the $U(1)_Y$ gauge boson with $B_\mu = c_W\,A_\mu + s_W\,Z_\mu$ and $W_{\mu\nu}^a$, $a = 1, 2, 3$, are field strength tensors of the $SU(2)_L$ gauge bosons with $W_\mu^3 = s_W\,A_\mu - c_W\,Z_\mu$ and A_μ (Z_μ) is photon (Z boson) field. The couplings y_{ij} are responsible for the LF violation and after the electroweak symmetry breaking we introduce modified couplings $\xi_{ij} = \frac{v}{\sqrt{2}}\,y_{ij}$ which respect the mass hierarchy of charged leptons. The process $l_i \to l_j\gamma$ appears in the tree level with the communication of two vertices[1] $\lambda_{ij}\,\frac{\xi_{ij}}{\Lambda_4^{d_U}}\,\bar{l}_i\,\sigma_{\mu\nu}\,l_j\,O_U^{\mu\nu}$ and $\left(2\,i\,\frac{g'\,c_W\,\lambda_B}{\Lambda_2^{d_U-2}} - i\,\frac{g\,v^2\,s_W\,\lambda_W}{2\,\Lambda_4^{d_U}}\right)k_\mu\,\epsilon_\nu\,O_U^{\mu\nu}$, by the antisymmetric tensor unparticle propagator (see Appendix and eq.(12)) and the matrix element of this process reads

$$M = a_{ij}\,\bar{l}_i\,\sigma_{\mu\nu}\,l_j\,k_\mu\,\epsilon_\nu\,, \tag{5}$$

where

$$a_{ij} = \frac{i\,e\,\mu^{2\,(d_U-2)}\;A_{d_U}\,\lambda_{ij}\,\xi_{ij}}{sin\,(d_U\pi)\,\Lambda_4^{d_U}}\left(\frac{\lambda_B}{\Lambda_2^{d_U-2}} - \frac{v^2\,\lambda_W}{4\,\Lambda_4^{d_U}}\right). \tag{6}$$

Finally the decay width $\Gamma(l_i \to l_j\gamma)$ becomes

$$\Gamma(l_i \to l_j\gamma) = \frac{1}{8\,\pi}\,m_i^3\,|a_{ij}|^2\,, \tag{7}$$

where m_i is the mass of incoming lepton. Notice that, in this expression, we ignore the mass of outgoing one.

[1]The first vertex arises from the last term of the effective lagrangian and leads to the $l_i \to l_j$ transition. The second one arises from the first and second terms of the effective lagrangian and results in the $O_U^{\mu\nu} \to A_\nu$ transition

Discussion

In this section we study the intermediate antisymmetric tensor unparticle contribution to the radiative LFV decays $l_i \to l_j \gamma$ which exist at tree level (see Fig.1). There are various free parameters in this scenario and we restrict them by using the current experimental upper limits of BRs of LFV decays. Now, we would like to present the free parameters and discuss the restrictions predicted. The SM sector interacts with the UV one and it appears as unparticle sector at a lower scale. The corresponding UV (unparticle) operator O_{UV} (O_U) has the scaling dimension d_{UV} (d_U) which is among the free parameters. We choose the scale dimension d_U in the range $1 < d_U < 2$. Notice that the scale dimension must satisfy $d_U > 2$ for antisymmetric tensor unparticle in order not to violate the unitarity [43]. Our assumption is based on the fact that the scale invariance is broken at some scale μ and one reaches to the particle sector. This results in a relaxation on the values of d_U and we choose d_U in the range $1 < d_U < 2$ so that the propagator for particle sector is obtained when d_U tends to one. Furthermore we choose the numerical value of d_{UV} as $d_{UV} = 3$ which satisfies $d_{UV} > d_U$ (see [40]). The SM-ultraviolet sector interaction scale M_U, the SM-unparticle sector interaction scale Λ_U and the scale μ which is the one that scale invariance is broken belong to the free parameter set of the present scenario. Here we choose $\mu \sim 1.0\, GeV$ and predict the restrictions for the others by using the experimental upper limits of LFV decays. Finally, for the couplings λ_B, λ_W and λ_{ij} we consider $\lambda_B = \lambda_W = \lambda_{ij} = 1$ and for ξ_{ij} we respect the mass hierarchy of charged leptons, namely we choose $\xi_{\tau\mu} > \xi_{\tau e} > \xi_{\mu e}$ and we take $\xi_{\tau\mu} = 0.1\, GeV$, $\xi_{\tau e} = 0.01\, GeV$ and $\xi_{\mu e} = 0.001\, GeV$ in our numerical calculations.

In Fig.2, we present the BR($\mu \to e\,\gamma$) with respect to the mass scale M_U for $r_U = \frac{\Lambda_U}{M_U} = 0.1$. Here, the solid (long dashed-short dashed) line represents the BR for $d_U = 1.7\,(1.8 - 1.9)$. We observe that the BR is sensitive to the mass scale M_U especially for the large values of the scale dimension d_U and it decreases almost three orders in the range of $2000\, GeV < M_U < 10000\, GeV$. The experimental upper limit is reached for $d_U \sim 1.8\,(1.9)$ and $M_U \sim 8000\,(4500)\, GeV$. Fig.3 is devoted to the BR($\mu \to e\,\gamma$) with respect to the scale parameter d_U for $r_U = 0.1$. Here the solid (long dashed-short dashed-dotted) line represents the BR for $M_U = 3000\,(5000 - 8000 - 10000)\, GeV$. The BR strongly depends on d_U and decreases with the increasing values of d_U. The experimental upper limit is observed in the range of $d_U \sim 1.78 - 1.88$ for $M_U \sim 5000 - 10000\, GeV$.

In Fig.4 we show the parameter r_U with respect to d_U for BR($\mu \to e\,\gamma$) $= 2.4 \times 10^{-12}$. Here

the solid (long dashed-short dashed) line represents r_U for $M_U = 5000\,(8000 - 10000)\,GeV$. We see that the scale dimension d_U and r_U can take values in the range $1.73 - 1.90$ and $0.05 - 0.12$, respectively for $M_U = 5000\,GeV$. For $M_U = 10000\,GeV$ we have the range $1.65 - 1.9$ for d_U and $0.05 - 0.20$ for r_U.

Fig.5 represents the BR($\tau \to e\,\gamma$) with respect to the mass scale M_U. Here, the solid (long dashed-short dashed-dotted) line represents the BR for $r_U = 0.1$, $d_U = 1.3$ ($r_U = 0.1$, $d_U = 1.4$-$r_U = 0.5$, $d_U = 1.6$-$r_U = 0.5$, $d_U = 1.7$). It is observed that the sensitivity of the BR to the mass scale M_U increases with the increasing values of the ratio r_U. The experimental upper limit is reached for $r_U = 0.1$ and $d_U \sim 1.3$ when the mass scale M_U reads $M_U \sim 4000\,GeV$. For $r_U = 0.5$ one reaches the experimental limit in the case of $d_U \sim 1.6$ and $M_U \sim 4000\,GeV$. Fig.5 shows the BR($\tau \to e\,\gamma$) with respect to the scale parameter d_U for $r_U = 0.1$. Here the solid (long dashed-short dashed) line represents the BR for $M_U = 2000\,(5000 - 10000)\,GeV$. The BR strongly depends on d_U and decreases with the increasing values of d_U similar to the $\mu \to e\,\gamma$ decay. One reaches the experimental upper limit in the range of $d_U \sim 1.26 - 1.32$ for $M_U \sim 2000 - 10000\,GeV$.

Fig.7 is devoted to the parameter r_U with respect to d_U for BR($\tau \to e\,\gamma$) $= 3.3 \times 10^{-8}$. Here the solid (long dashed-short dashed) line represents r_U for $M_U = 5000\,(8000 - 10000)\,GeV$. This figure shows that the experimental upper limit is reached for $M_U = 5000\,GeV$ if the scale dimension d_U and r_U can take values in the range $1.10 - 1.68$ and $0.05 - 1.00$, respectively. For $M_U = 10000\,GeV$ we have the range $1.10 - 1.64$ for d_U and $0.05 - 1.00$ for r_U.

In Fig.8, we present the BR($\tau \to \mu\,\gamma$) with respect to the mass scale M_U for $r_U = 0.1$. Here, the solid (long dashed-short dashed-dotted) line represents the BR for $d_U = 1.4\,(1.5 - 1.6 - 1.7)$. We observe that the BR decreases more than one order in the range of $2000\,GeV < M_U < 10000\,GeV$. The experimental upper limit is reached for $d_U \sim 1.4$ and $M_U \sim 9000\,GeV$. Fig.9 represents the BR($\tau \to \mu\,\gamma$) with respect to the scale parameter d_U for $r_U = 0.1$. Here the solid (long dashed-short dashed) line represents the BR for $M_U = 2000\,(5000 - 10000)\,GeV$. The experimental upper limit of the BR is observed in the range of $d_U \sim 1.38 - 1.47$ for $M_U \sim 2000 - 10000\,GeV$.

In Fig. 10 we show the parameter r_U with respect to d_U for BR($\tau \to \mu\,\gamma$) $= 4.4 \times 10^{-8}$. Here the solid (long dashed-short dashed) line represents r_U for $M_U = 2000\,(5000 - 10000)\,GeV$. We see that the scale dimension d_U and r_U can take values in the range $1.48 - 1.80\,(1.3 - 1.8)$ and $0.10 - 0.55\,(0.05 - 1.00)$, respectively for $M_U = 2000\,(5000)\,GeV$. For $M_U = 10000\,GeV$ we have the range $1.30 - 1.75$ for d_U and $0.05 - 1.00$ for r_U.

As a summary, the BRs of radiative LFV decays are sensitive to the mass scale M_U especially for the large values of the scale dimension d_U and this sensitivity increases with the increasing values of the ratio r_U. The experimental upper limit of the BR($\mu \to e\,\gamma$) can be reached for $r_U \sim 0.1$, $d_U > 1.7$ and for larger values of M_U, namely $M_U \sim 7000 - 9000\,GeV$. For BR($\tau \to e\,\gamma$) one reaches the experimental upper limit for $r_U \sim 0.1$, $d_U \sim 1.3$ and $M_U > 2000\,GeV$. If we consider the $\tau \to \mu\,\gamma$ decay the experimental upper limit of BR is obtained for $r_U \sim 0.1$, when d_U is in the range $d_U \sim 1.4 - 1.5$ and $M_U > 2000\,GeV$. We see that the free parameters of this scenario are more restricted if the $\mu \to e\,\gamma$ decay is considered. However the future more accurate measurements of the upper limits of the LFV decays make it possible to obtain a more restricted range for the free parameters of this scenario and they stimulate to search the role and the nature of unparticle physics which is a candidate to drive the lepton flavor violation.

Appendix

The scalar unparticle propagator reads [38, 44]

$$\int d^4x\, e^{ip.x} < 0|T\Big(O_U(x)\, O_U(0)\Big)0 >= i\frac{A_{d_U}}{2\,\pi}\, \int_0^\infty ds\, \frac{s^{d_U-2}}{p^2-s+i\epsilon} = i\, \frac{A_{d_U}}{2\, sin\,(d_U\pi)}\, (-p^2-i\epsilon)^{d_U-2} \quad (8)$$

where the factor A_{d_U} is

$$A_{d_U} = \frac{16\,\pi^{5/2}}{(2\,\pi)^{2\,d_U}}\, \frac{\Gamma(d_U+\frac{1}{2})}{\Gamma(d_U-1)\,\Gamma(2\,d_U)}\,. \quad (9)$$

Now the tensor unparticle propagator is obtained by using the projection operator $\Pi^{\mu\nu\alpha\beta}$

$$\Pi_{\mu\nu\alpha\beta} = \frac{1}{2}(g_{\mu\alpha}\, g_{\nu\beta} - g_{\nu\alpha}\, g_{\mu\beta})\,, \quad (10)$$

with the transverse and the longitudinal parts

$$\Pi^T_{\mu\nu\alpha\beta} = \frac{1}{2}(P^T_{\mu\alpha}\, P^T_{\nu\beta} - P^T_{\nu\alpha}\, P^T_{\mu\beta})\,, \quad \Pi^L_{\mu\nu\alpha\beta} = \Pi_{\mu\nu\alpha\beta} - \Pi^T_{\mu\nu\alpha\beta}\,, \quad (11)$$

where $P^T_{\mu\nu} = g_{\mu\nu} - p_\mu\, p_\nu/p^2$ (see for example [35] and references therein) and the propagator of antisymmetric tensor unparticle becomes

$$\int d^4x\, e^{ipx} < 0|T\Big(O^{\mu\nu}_U(x)\, O^{\alpha\beta}_U(0)\Big)0 >= i\, \frac{A_{d_U}}{2\, sin\,(d_U\pi)}\, \Pi^{\mu\nu\alpha\beta}(-p^2-i\epsilon)^{d_U-2}\,.$$

On the other hand the propagator is modified if the scale invariance broken at a certain scale and this modification is model dependent. Following the the simple model [41, 45, 46] we take

$$\int d^4x\, e^{ipx} < 0|T\Big(O^{\mu\nu}_U(x)\, O^{\alpha\beta}_U(0)\Big)0 >= i\, \frac{A_{d_U}}{2\, sin\,(d_U\pi)}\, \Pi^{\mu\nu\alpha\beta}(-(p^2-\mu^2)-i\epsilon)^{d_U-2}\,. \quad (12)$$

where μ is the scale that the scale invariance broken and the particle sector comes out.

References

[1] J. Adam et.al., MEG Collaboration, hep-ex/1107.5547, (2011).

[2] M. L. Brooks et. al., MEGA Collaboration, *Phys. Rev. Lett.* **83**, 1521 (1999).

[3] B. Aubert et. al., BABAR Collaboration, BABAR-PUB-09/026, SLAC-PUB-13753, *Phys. Rev. Lett.* **104** 021802, (2010).

[4] E. O. Iltan, *Phys. Rev.* **D64** 115005, (2001).

[5] E. O. Iltan,*Phys. Rev.* **D64** 013013, (2001)

[6] R. Diaz, R. Martinez and J-Alexis Rodriguez, Phys.Rev. D63 095007, (2001).

[7] E. O. Iltan, *JHEP* **0402** 20, (2004).

[8] E. O. Iltan, *JHEP* **0408** 20, (2004)

[9] E. O. Iltan, *Mod. Phys. Lett.* **A22** 819, (2007).

[10] E. O. Iltan, *Int. J. Mod. Phys.* **A23** 1055, (2008).

[11] R. Barbieri and L. J. Hall, *Phys. Lett.* **B338** 212, (1994).

[12] R. Barbieri, L. J. Hall and A. Strumia, *Nucl. Phys.* **B445** 219, (1995).

[13] R. Barbieri, L. J. Hall and A. Strumia, *Nucl. Phys.* **B449** 437, (1995).

[14] P. Ciafaloni, A. Romanino and A. Strumia, IFUP-YH-42-95.

[15] T. V. Duong, B. Dutta and E. Keith, *Phys. Lett.* **B378** 128, (1996).

[16] G. Couture, et. al., *Eur. Phys. J.* **C7** 135, (1999).

[17] Y. Okada, K. Okumara and Y. Shimizu, *Phys. Rev.* **D61** 094001, (2000).

[18] S. Khalil, *Phys. Rev.* **D81** 035002, (2010).

[19] D. Chang, W. S. Hou and W. Y. Keung, *Phys. Rev.* **D48** 217, (1993).

[20] P. Paradisi, *JHEP* **0602** 050, (2006).

[21] G. J. Ding, M. L. Yan, *Phys. Rev.* **D77** 014005, (2008).

[22] A. Hektor, Y. Kajiyama, K. Kannike, *Phys. Rev.* **D78** 053008, (2008).

[23] F. del Aguila, J. I. Illana, M. D. Jenkins, *JHEP* **0901** 080, (2009).

[24] J. I. Illana, M. D. Jenkins, *Acta Phys. Polon.* **B40** 3143, (2009).

[25] T. Goto, Y. Okada, Y. Yamamoto, *Phys. Rev.* **D83** 053011, (2011).

[26] F. del Aguila, J. I. Illana, M. D. Jenkins, *JHEP* **1103** 080, (2011).

[27] X. G. He, S. Oh, *JHEP* **0909** 027, (2009).

[28] D. Ibanez, S. Morisi, J.W.F. Valle, *Phys. Rev.* **D80** 053015, (2009).

[29] C. Hagedorn, E. Molinaro, S. T. Petcov, *JHEP* **1002** 047, (2010).

[30] F. F. Deppisch, F. Plentinger, G. Seidl, *JHEP* **1101** 004, (2011).

[31] G. J. Ding, J. F. Liu , *JHEP* **1105** 029, (2010).

[32] J.I. Aranda, A. F. Tlalpa, F. R. Zavaleta , F. J. Tlachino, J. J. Toscano, E. S. Tututi, *Phys. Rev.* **D79** 093009, (2009).

[33] A. G. Akeroyd, M. Aoki, H. Sugiyama, *Phys. Rev.* **D79** 113010, (2009).

[34] A. Goudelis, O. Lebedev, J. H. Park, hep-ph/1111.1715, (2011).

[35] T. Hur, P. Ko, X. H. Wu, *Phys. Rev.* **D76**, 096008 (2007)

[36] E. Iltan, *J. Phys.* **G38** , 105001 (2011).

[37] H. Georgi, *Phys. Rev. Lett.* **98**, 221601 (2007).

[38] H. Georgi, *Phys. Lett.* **B650**, 275 (2007).

[39] T. Banks, A. Zaks, *Nucl. Phys.* **B196**, 189 (1982).

[40] M. Bander, J. L. Feng, A. Rajaraman, Y. Shirman, *Phys. Rev.* **D76**, 115002 (2007).

[41] P. J. Fox, A. Rajaraman, Y. Shirman, *Phys. Rev.* **D76**, 075004 (2007).

[42] T. Kikuchi, N. Okada, *Phys. Lett.* **B661**, 360 (2008).

[43] B. Grinstein, K. A. Intriligator, I. Z. Rothstein *Phys. Lett.* **B662**, 367 (2008).

[44] K. Cheung, W. Y. Keung and T. C. Yuan, *Phys. Rev.* **D76**, 055003 (2007)..

[45] A. Rajaraman, *Phys. Lett.* **B671**, 411 (2009).

[46] A. Delgado, J. R. Espinosa, J. M. No and M. Quiros, *JHEP* **0804**, 028 (2008)

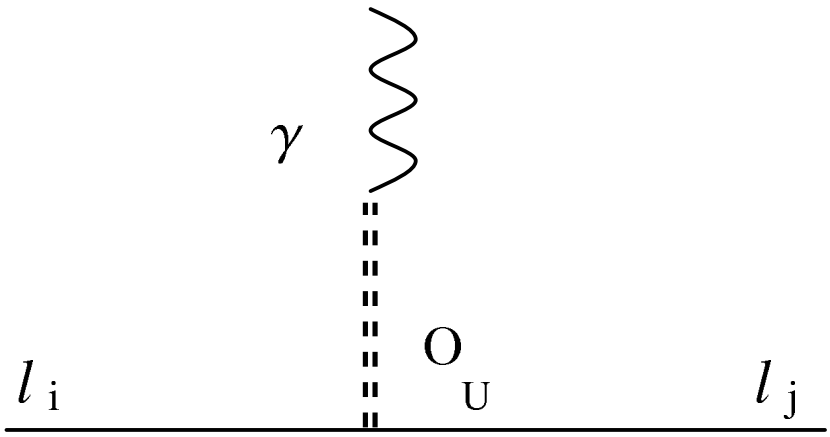

Figure 1: Tree level diagram contributing to the $l_i \to l_j\,\gamma$ decay due to antisymmetric tensor unparticle. Wavy (solid) line represents the electromagnetic field (lepton field) and double dashed line the antisymmetric tensor unparticle field.

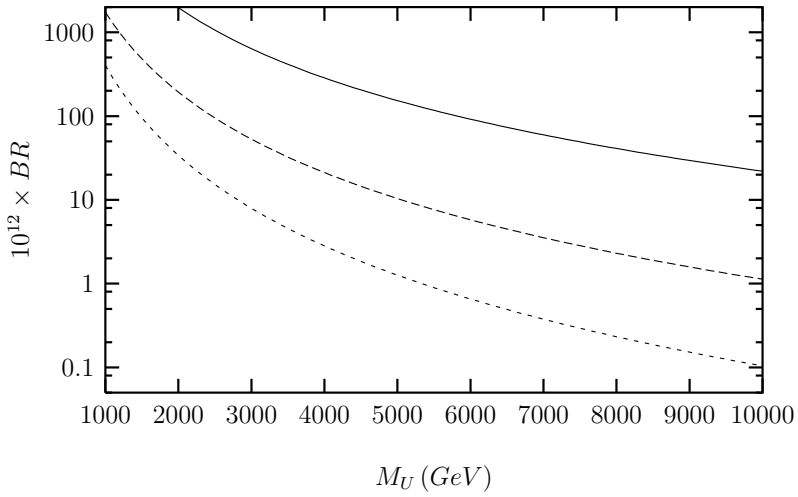

Figure 2: M_U dependence of the BR $(\mu \to e\,\gamma)$ for $r_U = 0.1$. Here, the solid (long dashed-short dashed) line represents the BR for $d_U = 1.7\,(1.8 - 1.9)$.

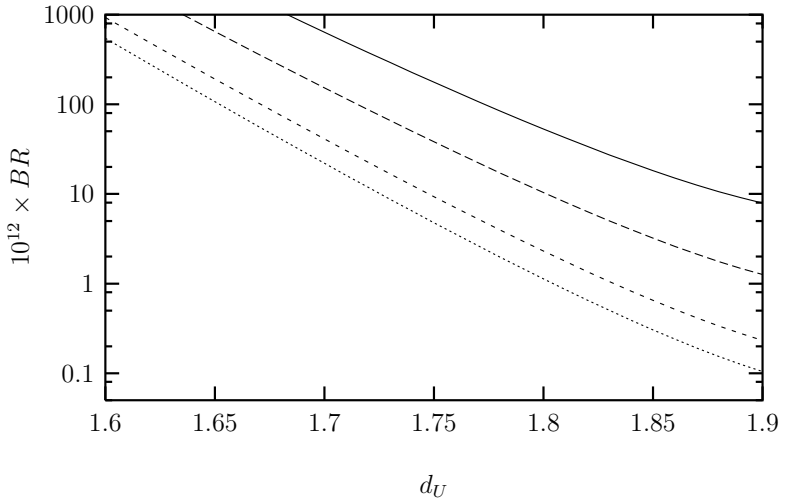

Figure 3: d_U dependence of the BR $(\mu \to e\,\gamma)$ for $r_U = 0.1$. Here the solid (long dashed-short dashed-dotted) line represents the BR for $M_U = 3000\,(5000 - 8000 - 10000)\,GeV$.

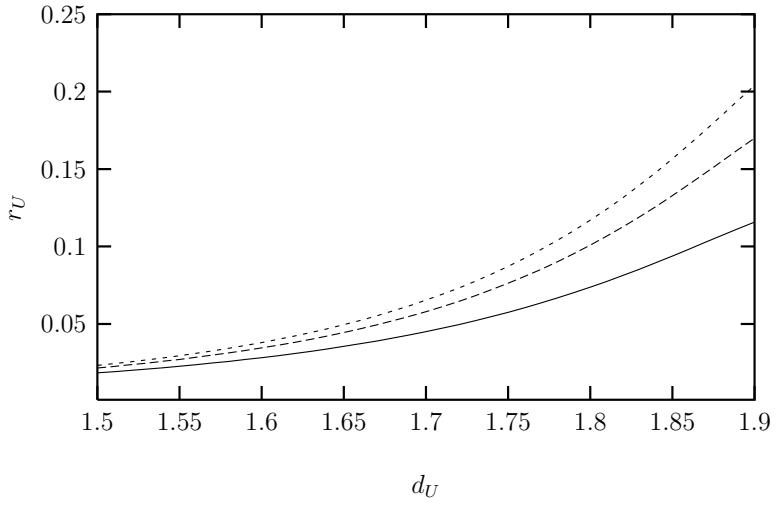

Figure 4: r_U with respect to d_U for BR($\mu \to e\,\gamma$) = 2.4×10^{-12}. Here the solid (long dashed-short dashed) line represents r_U for $M_U = 5000\,(8000 - 10000)\,GeV$

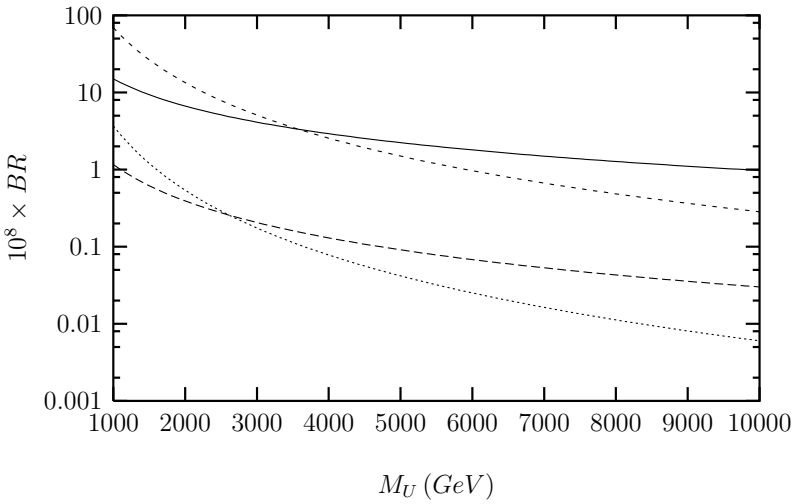

Figure 5: M_U dependence of the BR ($\tau \to e\,\gamma$). Here, the solid (long dashed-short dashed-dotted) line represents the BR for $r_U = 0.1$, $d_U = 1.3$ ($r_U = 0.1$, $d_U = 1.4$-$r_U = 0.5$, $d_U = 1.6$-$r_U = 0.5$, $d_U = 1.7$).

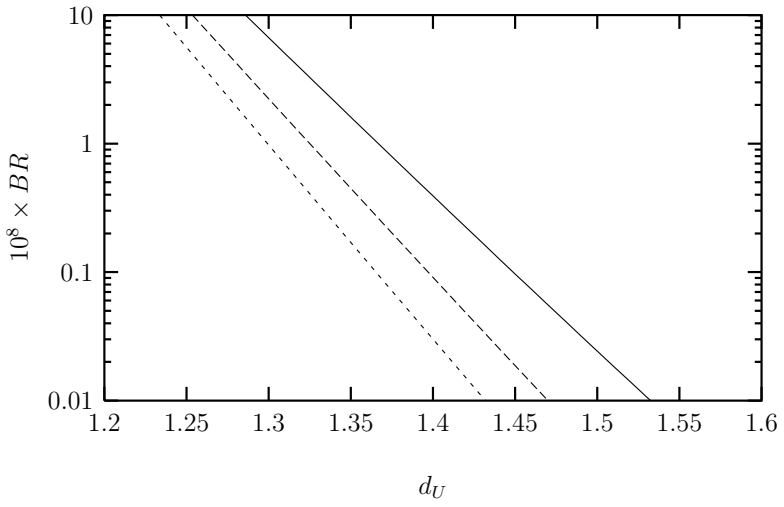

Figure 6: d_U dependence of the BR ($\tau \to e\,\gamma$) for $r_U = 0.1$. Here the solid (long dashed-short dashed) line represents the BR for $M_U = 2000\,(5000 - 10000)\,GeV$.

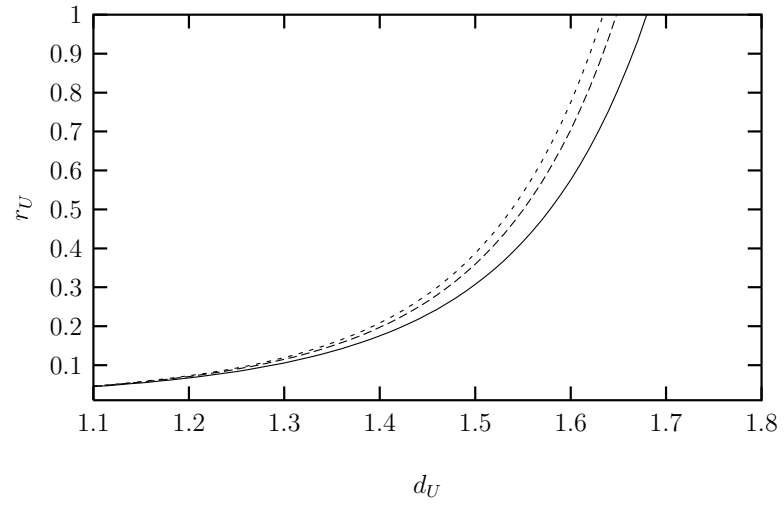

Figure 7: r_U with respect to d_U for BR($\tau \to e\,\gamma$) $= 3.3 \times 10^{-8}$. Here the solid (long dashed-short dashed) line represents r_U for $M_U = 5000\,(8000 - 10000)\,GeV$.

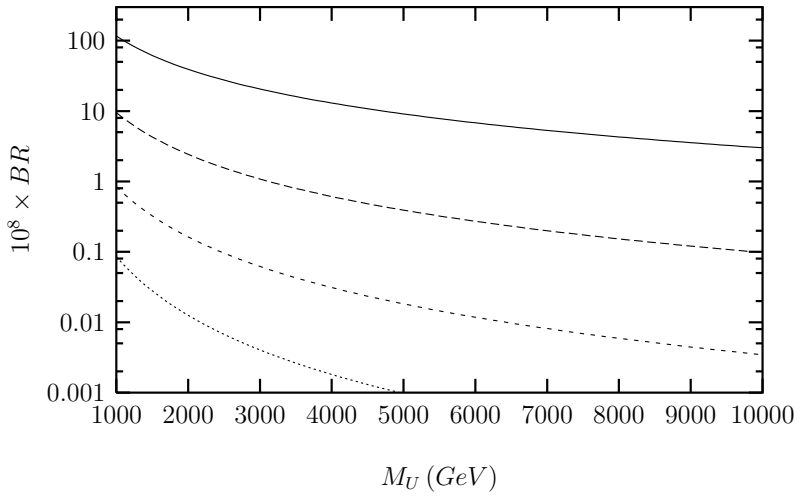

Figure 8: M_U dependence of the BR($\tau \to \mu\,\gamma$). Here, the solid (long dashed-short dashed-dotted) line represents the BR for $d_U = 1.4\,(1.5 - 1.6 - 1.7)$.

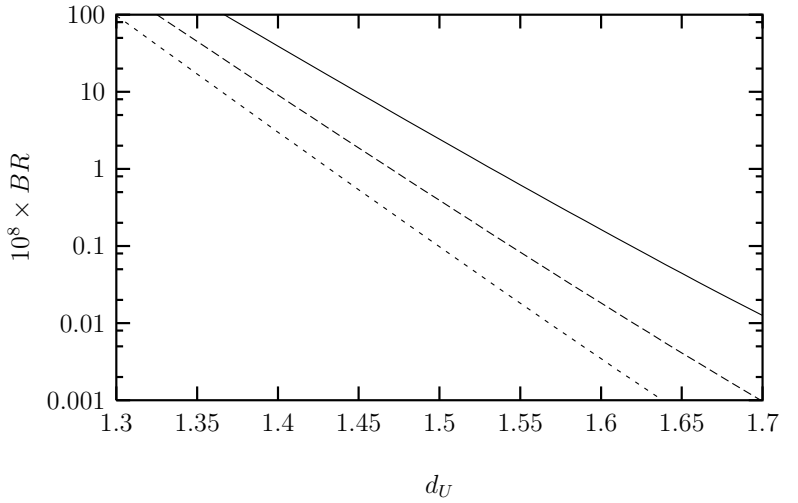

Figure 9: d_U dependence of the BR($\tau \to \mu\,\gamma$) for $r_U = 0.1$. Here the solid (long dashed-short dashed) line represents the BR for $M_U = 2000\,(5000 - 10000)\,GeV$.

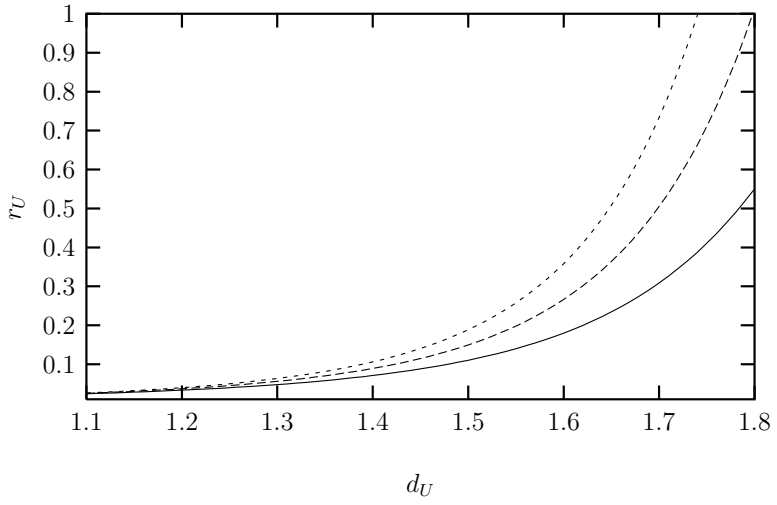

Figure 10: r_U with respect to d_U for $\mathrm{BR}(\tau \to \mu\,\gamma) = 4.4 \times 10^{-8}$. Here the solid (long dashed-short dashed) line represents r_U for $M_U = 2000\,(5000 - 10000)\,GeV$.